The EMBO Journal vol.5 no.6 pp.1181-1186, 1986

Binding of fluoresceinated epidermal growth factor to A431 cell sub-populations studied using a model-independent analysis of flow cytometric fluorescence data

R.C.Chatelier, R.G.Ashcroft, C.J.Lloyd, E.C.Nice, R.H.Whitehead, W.H.Sawyer[1] and A.W.Burgess

Ludwig Institute for Cancer Research, Melbourne Tumour Biology Branch, Post Office Royal Melbourne Hospital, Victoria 3050, and [1]The Russell Grimwade School of Biochemistry, University of Melbourne, Victoria 3052, Australia

Communicated by L.Philipson

A method is developed for determining ligand-cell association parameters from a model-free analysis of data obtained with a flow cytometer. The method requires measurement of the average fluorescence per cell as a function of ligand and cell concentration. The analysis is applied to data obtained for the binding of fluoresceinated epidermal growth factor to a human epidermoid carcinoma cell line, A431. The results indicate that the growth factor binds to two classes of sites on A431 cells: 4 x 10^4 sites with a dissociation constant (K_D) of $\leq$20 pM, and 1.5 x 10^6 sites with a K_D of 3.7 nM. A derived plot of the average fluorescence per cell versus the average number of bound ligands per cell is used to construct binding isotherms for four sub-populations of A431 cells fractionated on the basis of low-angle light scatter. The four sub-populations bind the ligand with equal affinity but differ substantially in terms of the number of binding sites per cell. We also use this new analysis to critically evaluate the use of 'Fluorotrol' as a calibration standard in flow cytometry.

Key words: isoparametric binding analysis/Scatchard plot/EGF receptors/'Fluorotrol'/fluorescence standard calibration

Introduction

The interaction of specific ligands with cell surfaces is of importance in fields such as immunology, endocrinology and the study of cell differentiation. Cell suspensions contain diverse cell types (e.g. dead cells, cells which are in various phases of the cell cycle and cellular debris) and conventional binding techniques are unable to discriminate between these cell sub-populations. When the ligand of interest is labelled with a fluorophore, it is possible to detect ligand-cell association using a flow cytometer which can differentiate between various cell types on the basis of their light scatter and fluorescence properties. Some procedures for measuring the number of binding sites on cells combine flow cytometry with steady-state fluorescence (Steinkamp and Kramer, 1979) or radiometric (Titus *et al.*, 1981) assays, while others employ fluorescent calibration standards (Sklar *et al.*, 1984). Recently, Sklar and Finney (1982) proposed a method, based on flow cytometry alone, for obtaining the number of binding sites and the binding constant without recourse to external standards. Their method is valid if, and only if, ligands of identical quantum yield bind to equivalent and independent sites on the cell.

In this report, we outline a procedure for obtaining formal thermodynamic information from a model-free 'isoparametric' analysis of flow cytometric data. The analysis will be applied to the binding of fluoresceinated epidermal growth factor (EGF-FITC) to A431 cells. Certain reports in the literature indicate that there is one class of binding sites for EGF on A431 cells (Fabricant *et al.*, 1977; Lifshitz *et al.*, 1983), while others demonstrate two classes of sites (Kawamoto *et al.*, 1983; Rees *et al.*, 1984). We re-examine this issue using the isoparametric analysis, and also determine the relative fluorescence quantum yields of successive ligands bound to the cell surface. We then explore the interaction of EGF-FITC with sub-populations of A431 cells which have been fractionated on the basis of their forward light scatter properties. Finally, we re-appraise alternative flow cytometric strategies for investigating ligand-cell associations.

Theory

Sklar and Finney (1982) observed that in equilibrated mixtures of cells and fluorescent ligand, under certain conditions of ligand and cell concentration, the flow cytometer measured only the cell-bound ligand fluorescence. A similar observation had been previously made by Watson *et al.* (1977) on the effects of leaking fluorescein from living cells loaded with fluorescein diacetate. The effect probably results from dilution of the free ligand concentration by the sheath fluid. The dilution occurs rapidly (10 ms) and hence will not perturb the ligand-cell equilibrium. The average fluorescence per cell of the total population (F_t) is obtained from the flow cytometric data by calibration of the photomultiplier tube and conversion of the mean signal from a logarithmic scale to a linear scale, followed by subtraction of the background autofluorescence.

Consider a plot of F_t versus total ligand concentration ($[L]_T$), at various cell concentrations ([C], expressed in molar units). At appropriately high cell concentrations, F_t will decrease due to a reduction in the binding function, r (= moles ligand bound per mole cells). An 'isoparametric principle' used in the analysis of fluorescence quenching (Encinas and Lissi, 1982; Blatt *et al.*, 1984) can be applied to this data. A given value of F_t will correspond to a unique value of r. Invoking the law of conservation of mass:

$$[L]_T = [L]_A + [L]_C \quad \text{(i)}$$

where $[L]_T$ and $[L]_C$ are the concentration of ligand in the aqueous phase and the cell, respectively, expressed relative to the total volume of the system. Since $[L]_C = r[C]$:

$$[L]_T = [L]_A + r[C] \quad \text{(ii)}$$

Thus a plot of $[L]_T$ versus [C], at a given value of F_t, is linear with slope r and ordinate intercept $[L]_A$. Repeating the analysis at several values of F_t allows the construction of a plot of r versus $[L]_A$ (or the commonly used Scatchard or double reciprocal plots) which can then be interpreted according to an appropriate thermodynamic model.

It is also possible to construct a plot of F_t versus r; this has three uses. Firstly, it will provide information on the fluorescence properties of the ligand (e.g a non-linear plot may be due to heterogeneous ligand environments). Secondly, it can be used

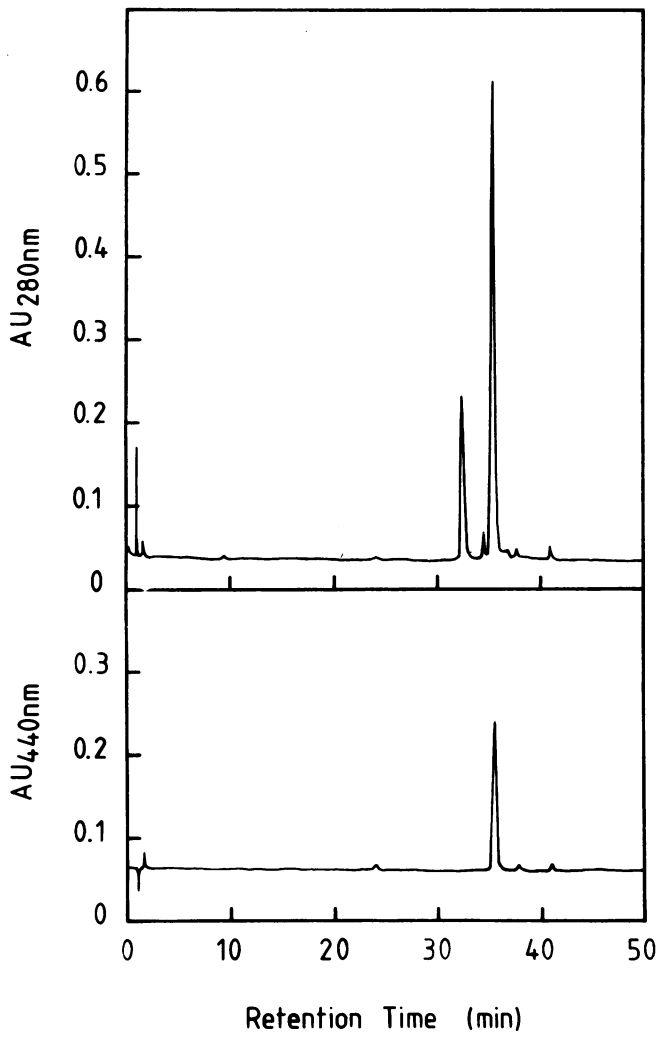

Fig. 1. H.p.l.c. purification of the EGF–FITC. EGF–FITC was purified from unreacted EGF by h.p.l.c. on an ODS-Hypersil column (150 × 4.6 mm i.d.). Chromatographic conditions are given in Materials and methods. **Upper panel**, detection at 280 nm. **Lower panel**, detection at 440 nm.

to correct binding data for 'non-specific' binding. An excess of unlabelled EGF is mixed with the EGF–FITC prior to the addition of cells. The value of F_t is used to obtain r by interpolation and hence $[L]_A = [L]_T - r[C]$. The non-specifically bound EGF–FITC is then subtracted from the total bound ligand at a given value of $[L]_A$. Thirdly, the plot of F_t versus r can be used to generate binding isotherms for cell sub-populations. The value of F_i for the ith sub-population is used to obtain the binding function for that sub-population (r_i) by interpolation. The corresponding value of $[L]_A$ is calculated using F_t to obtain the overall binding function and hence $[L]_A = [L]_T - r[C]$. We note that the fluorescence of each sub-population must be corrected using the autofluorescence of that sub-population, and that the binding function should also be corrected using the non-specific binding of each sub-population.

In summary, the average fluorescence of the total population is analysed, and plots of r versus $[L]_A$ and F_t versus r are generated. The latter plot can be used to correct the data for non-specific binding and to generate binding data for cell sub-populations.

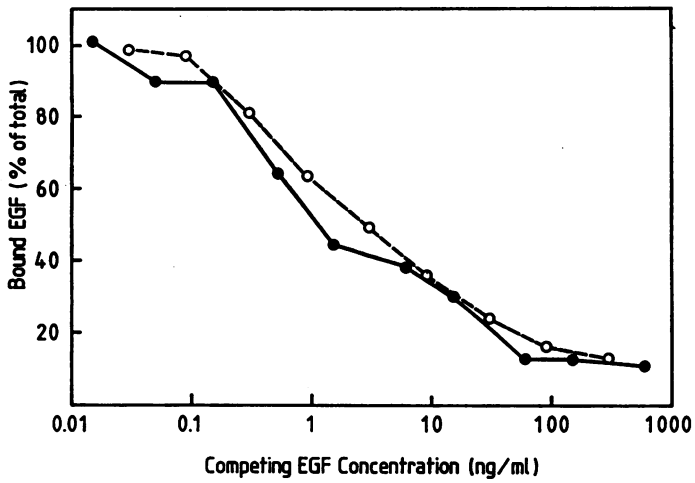

Fig. 2. Competition of EGF–FITC (●) and EGF (○) with [^{125}I]EGF for the EGF receptors on A431 cells.

Results

Separation of EGF–FITC from EGF

The coupling of EGF with FITC does not proceed to completion and it is therefore necessary to separate the EGF–FITC conjugate from the two reactants. Free FITC is readily removed from solution using a Sephadex G25 column. The separation of EGF–FITC from EGF is more difficult and is achieved using reversed-phase h.p.l.c. (Figure 1). The first peak represents EGF (retention time 32 min, 280 nm absorbance only) and the second denotes the conjugate (retention time 36 min, absorbing at both 280 and 440 nm). The shoulder in the second peak arises from an impurity which was present in the starting material. Approximately half of the EGF did not react with FITC, but purification of this component followed by addition of fresh FITC resulted in further conjugate formation.

Competitive, mitogenic and colony-forming assays of EGF and EGF–FITC

The relative binding affinity of the EGF and the EGF–FITC for the EGF receptors on A431 cells was determined using a competition assay as described in Materials and methods. Figure 2 shows that both species compete equally well with [^{125}I]EGF, indicating that the affinity of the EGF–FITC is identical to that of the native protein.

The biological activity of the EGF–FITC was measured by assaying the mitogenic response of BALB/c 3T3 cells and by the ability of normal rat kidney fibroblast (NRK) cells to form colonies in soft agar cultures (data not shown). Both methods showed the EGF and FITC-labelled EGF to be of equal potency.

Since we have a pure EGF–FITC conjugate which is biologically active and which has the same binding affinity as the native protein, it is appropriate to use this conjugate in quantitative flow cytometric binding studies.

Binding of EGF–FITC to A431 cells

Figure 3A shows plots of F_t versus $[L]_T$ for the association of EGF–FITC with A431 cells obtained at various cell concentrations. As the cell concentration increases, the aqueous phase is depleted of ligand, and the resulting decrease in the binding function is reflected in reduced values of F_t. Figure 3B shows this data re-plotted according to Equation 2 at various fixed values of F_t. The slope and ordinate intercept of each line represent the

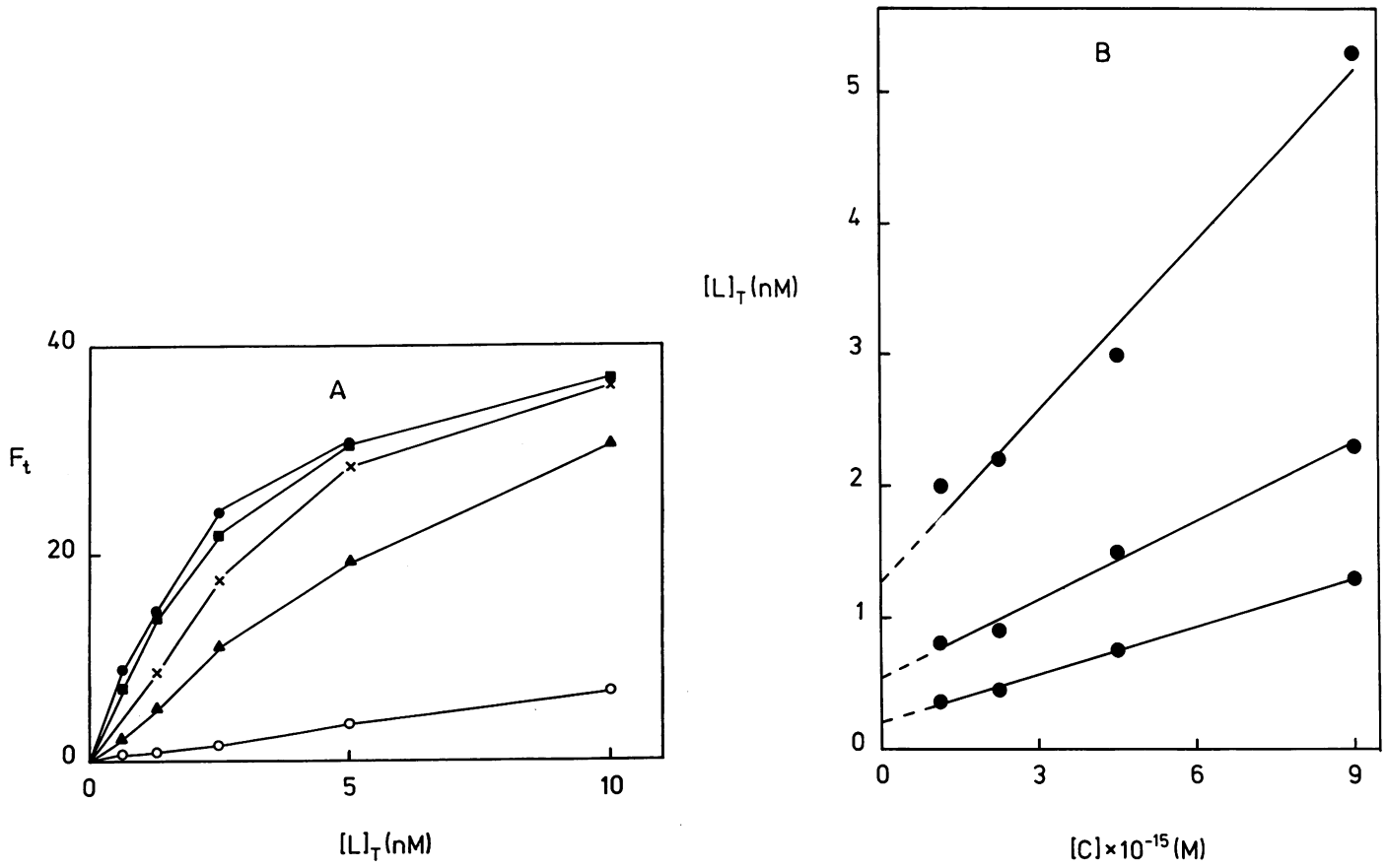

Fig. 3. (**A**) Plots of the average fluorescence per A431 cell versus the total concentration of EGF–FITC for various cell concentrations: 7×10^5/ml (●), 1.4×10^6/ml (■), 2.7×10^6/ml (X) and 5.4×10^6/ml (▲). Also shown is the non-specific binding when the cell concentration is 7×10^5/ml (○). The autofluorescence (equivalent to 6.7 units on the above scale) has been subtracted from each point. (**B**) Replot of data in **A** according to Equation 2. From top to bottom, values of F_t are 20, 10 and 15. The cell concentration was expressed in molar units by dividing the number of cells/litre by Avogadro's number.

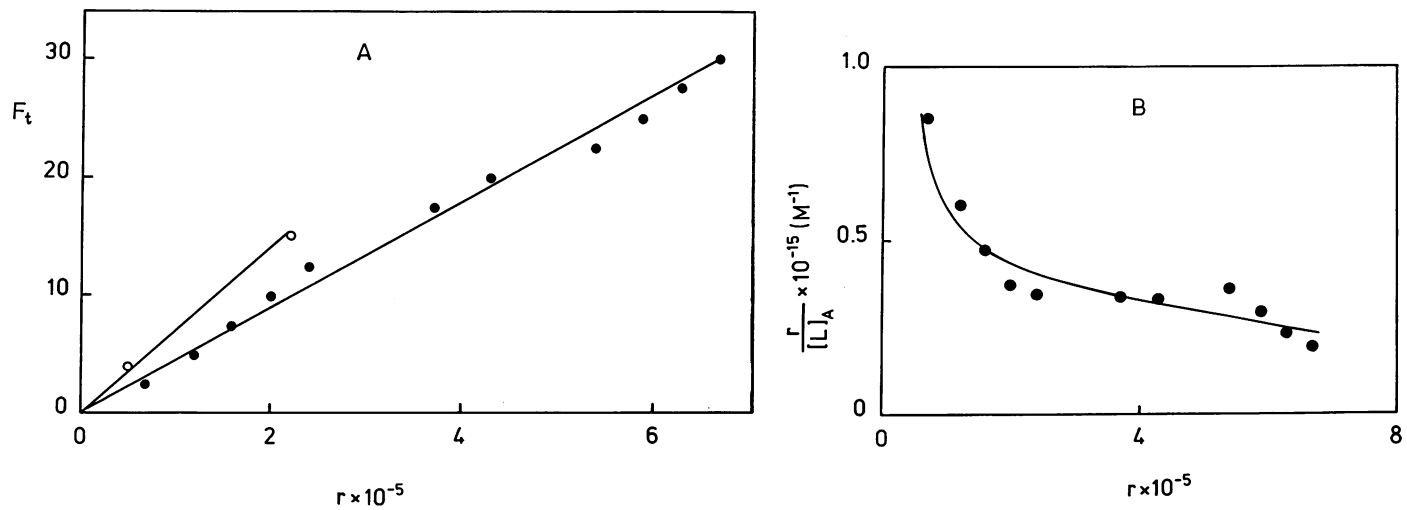

Fig. 4. (**A**) Plot of F_t versus r for EGF–FITC bound to A431 cells (●). Also shown is a plot of F_t versus the number of fluoresceins per thymocyte nucleus in the Fluorotrol standand (○). (**B**) Scatchard plot for the binding of EGF–FITC to A431 cells. Subtraction of the non-specific binding was carried out as described in the text.

binding function and free ligand concentration, respectively, corresponding to a given value of F_t.

There are two types of information which may be derived from this analysis: spectroscopic information, contained within a plot of F_t versus r, and thermodynamic information, obtainable by a Scatchard plot, $r/[L]_A$ versus r, or similar constructs.

Figure 4A shows a plot of the average fluorescence per cell versus the binding function. The plot is approximately linear, indicating that each added ligand results in an equal increment in the fluorescence signal.

The Scatchard plot displayed in Figure 4B indicates that EGF–FITC binds to two classes of sites on A431 cells. These

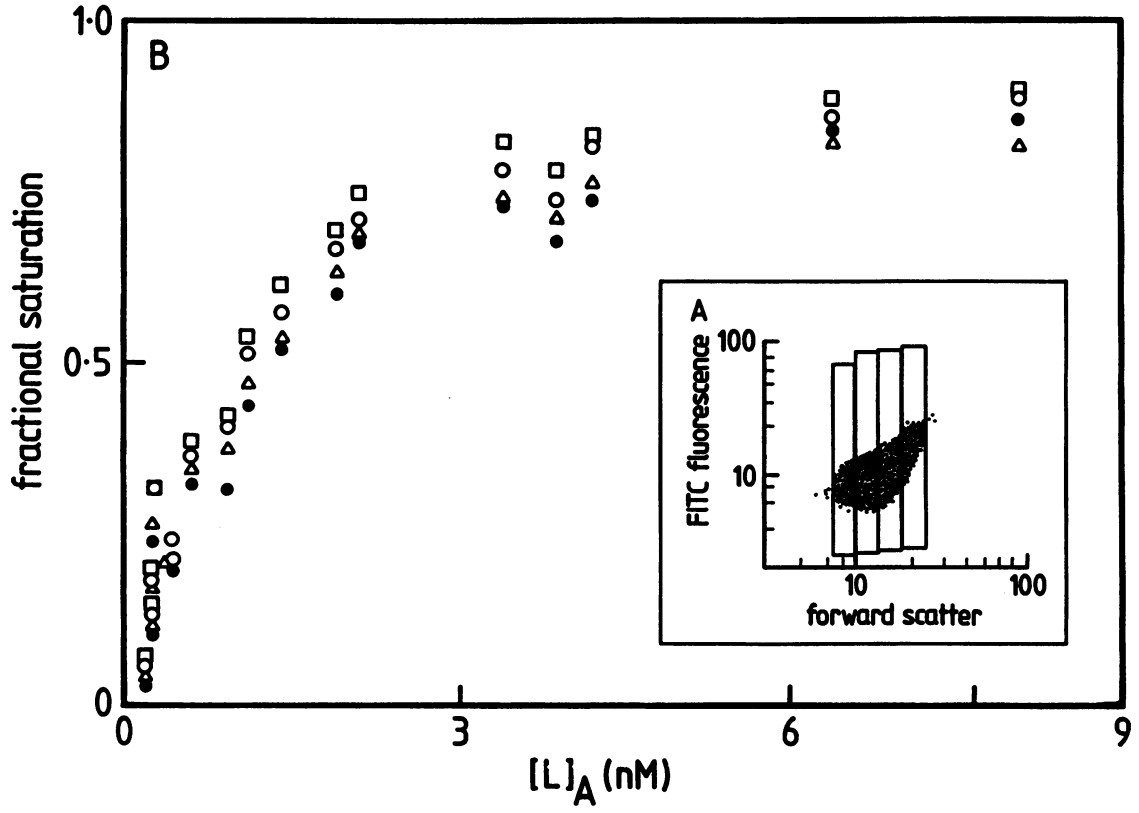

Fig. 5. (**A**) Plot of log fluorescence versus log low-angle scatter. An increase of 15 channels represents a doubling of the fluorescence signal. Four gated regions are also shown. (**B**) Plot of the fractional saturation of binding sites versus $[L]_A$ for each of the four cell sub-populations delineated in **B**. Sub-population 1 (○), 2 (△), 3 (□) and 4 (●), defined as left to right, 1–4, in **A**.

data were fitted to the equation:

$$r = p_1K_1[L]_A/(1+K_1[L]_A) + p_2K_2[L]_A/(1+K_2[L]_A) \quad \text{(iii)}$$

where p_1 and p_2 represent the number of sites per cell in class 1 and class 2, respectively, and K_1 and K_2 are the corresponding association constants. The data points were weighted according to Koeppe and Hamann (1980) during an iterative least squares minimization procedure. The best fit values are $p_1 = 4 \times 10^4$, $K_1 \geq 5 \times 10^{10}$/M, $p_2 = 1.5 \times 10^6$ and $K_2 = 2.7 \times 10^8$/M.

Is 'Fluorotrol' an appropriate calibration standard?

'Fluorotrol' (a generous gift of Dr D.Burger, Ortho Diagnostics Inc.) consists of a mixture of calf thymocyte nuclei stained with 0, 50 000 and ~220 000 FITC molecules. It has been used to calibrate a flow cytometer in order to measure the number of fluorophores bound per cell (Sklar *et al.*, 1984). Such a procedure assumes that the quantum yield of the fluorescein molecules in 'Fluorotrol' is identical to that of the fluorescein derivative associated with the cell. We test this assumption in Figure 4A, where the average fluorescence per thymocyte nucleus is plotted against the number of fluoresceins per nucleus. The slope of this line is 1.6-fold steeper than the slope of the corresponding line obtained for EGF–FITC bound to A431 cells. The average quantum yield of the fluorescein in 'fluorotrol' is thus 1.6-fold greater than that of the fluorescein in cell-bound EGF–FITC. Ignoring this effect leads to systematic errors in estimates of p and K.

Binding to cell sub-populations

Figure 5A displays a plot of the logarithm of the right-angle fluorescence of EGF–FITC bound to A431 cells versus the logarithm of the low-angle scatter of the cells. The fluorescence per cell typically varies 8- to 10-fold in the population. Does this differential binding of ligand represent a difference in the number of receptors per cell or in the binding affinity? We sought to answer this question using the plot of F_t versus r in Figure 4A to construct Scatchard plots for each of the four sub-populations depicted in Figure 5A. These plots (not shown) revealed that the total number of sites ($p_1 + p_2$) increased in the ratio 1:1:1.3:2.4 as the low-angle scatter increased. Plots of the fractional saturation $[r_i/(p_1+p_2]$ versus $[L]_A$ (Figure 5B) demonstrate the similar affinity of all four sub-populations for the ligand. A duplicate experiment confirmed that A431 cell sub-populations had similar affinities for EGF–FITC, and that the differential binding was due to differences in the numbers of sites/cell in each of the sub-groups.

Discussion

The contribution of this paper lies in the marriage of a model-independent 'isoparametric' analysis with the ability of a flow cytometer to resolve cell sub-populations. The isoparametric analysis has several advantages. Firstly, no thermodynamic or spectroscopic assumptions are required in order to construct a Scatchard plot. Secondly, formal (rather than 'apparent') association parameters are reported. Thirdly, the analysis is fairly insensitive to random experimental error since the plot of $[L]_T$ versus [C] smoothes the noise in the data. Fourthly, the isoparametric method may be used to calibrate commercially available flow cytometric standards such as Fluorotrol.

How do the binding parameters obtained by the isoparametric analysis compare with published studies? Rees *et al.* (1984) report $p_1 = 1.6 \times 10^5$, $K_1 = 10^9$/M, $p_2 = 1.7 \times 10^6$ and $K_2 = 10^8$/M,

in reasonable agreement except that our value of K_1 is higher. As discussed in the Introduction, however, the binding parameters reported in the literature vary widely both qualitatively (number of classes of sites) and quantitatively (number of sites per cell, association constant). Such variation may be due to 'differential ageing' of the cell lines, or to differences in growth conditions (Gill and Lazar, 1981).

Conventional binding techniques measure the interaction of a ligand with all cell types present and therefore report the average number of sites (Walker and Burgess, 1985). A flow cytometer, however, is able to distinguish various cell sub-populations such as 'binding' and 'non-binding' cells. We used low-angle (forward) light scatter to gate regions of the cytogram. There is a rough correlation between low-angle scatter and cell size, and therefore the finding that the total number of sites increases with increasing low-angle scatter simply implies that larger cells have more receptors. It is difficult to comment on the receptor surface density in each sub-population because the exact relationship between low-angle scatter and surface area is unknown.

The cell population depicted in Figure 5A is presumably composed of cells from various phases of the cell cycle and we would expect that Region 1 contains more cells in G1 than G2 whereas the opposite is true of Region 4. The finding that all four sub-populations have the same affinity suggests that the affinity of the EGF receptor for EGF–FITC does not vary substantially during the cell cycle.

Many spectroscopic analyses assume that there is a linear relationship between the measured signal and the number of bound ligands. The linearity of the plot of F_t versus r in Figure 4A demonstrates that this is indeed the case for the binding of EGF–FITC to A431 cells. However, non-linear plots may arise if there is substantial resonance energy transfer between proximal fluorescent ligands, or if the ligands bind to non-equivalent sites of varying polarity or adjacent to heterogeneous quenching groups on the acceptor. We emphasize, however, that the isoparametric analysis is independent of the type of relationship between F_t and r.

The use of 'Fluorotrol' as a calibration standard in flow cytometry rests on two assumptions. Firstly, all bound ligands must have identical quantum yields. This assumption may be tested by assessing the linearity of the plot of F_t versus r. If the plot is non-linear, then 'Fluorotrol' cannot be used as a calibration standard. Secondly, the quantum yield of the bound ligands must be the same as that of the fluorescein residues in 'Fluorotrol'. This may be tested by comparing the slope of the plot of F_t versus r with the fluorescence per fluorescein residue in 'Fluorotrol'. If the two differ, then the isoparametric analysis can be used to calibrate the 'Fluorotrol' standard.

Materials and methods

Murine $EGF_{\alpha 1}$ was prepared from adult male mouse salivary glands by h.p.l.c. as described previously (Burgess *et al.*, 1983). The conjugate to fluorescein isothiocyanate (EGF–FITC) was prepared by mixing 50 μl of EGF solution [2.7 mg/ml EGF in trifluoroacetic acid (TFA)/acetonitrile/water (0.2%/50%/49.8%)] with 50 μl of FITC solution (20 mg/ml in dimethylsulphoxide) and 10 μl of 0.1 M $KHCO_3$, then incubating the mixture for 1 h at room temperature.

Unreacted FITC was separated from higher mol. wt protein components (unreacted EGF and EGF–FITC) using a Sephadex G25 column (Pharmacia South Seas, Sydney), the conjugate eluted at the void volume. The EGF was resolved from the EGF–FITC by h.p.l.c. using a Beckman Model 324-40 liquid chromatograph fitted with a Model 210 septumless injection valve with a 2 ml sample loop. Proteins were separated at ambient temperature and a flow-rate of 1 ml/min on a 150 × 4.6 mm i.d. column packed with ODS-Hypersil (5 μm, 12 nm octadecylsilane-bonded silica, Shandon Southern Products, UK). The column was developed with a linear 50 min gradient between a primary solvent of 0.2% (v/v) aqueous TFA and a secondary solvent identical to that used for preparing the EGF solution for reaction with FITC. Eluting proteins were detected at 280 nm using a Spectromonitor III variable wavelength detector (SGE, Melbourne, Australia). EGF–FITC was specifically monitored at 440 nm using a second detector 'on line'. Fractions were recovered using a FRAC 100 collector (Pharmacia, Uppsala, Sweden). EGF–FITC concentrations were determined by amino acid analysis using a Beckman Model 6300 analyser.

A431 cells for flow cytometric studies were cultured at 37°C in RPMI 1640 medium containing 10% foetal calf serum (Gibco New Zealand Ltd). They were harvested at ~90% confluence by exposure to 8 mM EDTA in phosphate buffered saline (PBS) for 15 min at 37°C (Zidovetzki *et al.*, 1981), and were washed and resuspended in PBS containing 0.1% bovine serum albumin (BSA) and 0.02% sodium azide. Cell concentrations were determined in a Coulter Counter.

Cellular fluorescence was measured using an ORTHO System 50H cytofluorograf (Ortho Diagnostics Inc., Westwood, MA, USA). Excitation was at 488 nm using an Argon laser, and the fluorescence emission was collected between 518 and 538 nm using the standard fluorescein filter. The fluorescence, low-angle scatter and right-angle scatter properties of 20 000 cells were stored on disk in the System 2150 data acquisition computer (Ortho Diagnostics Inc.) prior to being processed.

Flow cytometric binding studies were performed at 0°C in PBS containing 0.1% BSA and 0.02% azide. Appropriate concentrations of 200 μl cell suspension and 50 μl EGF–FITC were mixed such that the final cell concentration varied between 0.4 and 6 × 10^6/ml and the final EGF–FITC concentration between 1 and 40 nM. In some cases, 10 μl of 27 μM unlabelled EGF was mixed with the EGF–FITC prior to the addition of cells in order to assess the level of non-specific binding. Autofluorescence blanks (where 50 μl buffer replaced the EGF–FITC) were also prepared. All samples were placed on ice in the dark for 2 h prior to the measurement of cellular fluorescence.

The relative binding affinity of the EGF and the EGF–FITC for EGF receptors was determined using A431 cells and [^{125}I]EGF in a competition experiment. The assay was performed with adherent cells (2.5 × 10^5 per well of a 24 well 16 mm cluster dish) in 1 ml of Dulbecco's modified Eagles medium (DMEM) containing 0.1% BSA and 0.02% sodium azide. Cells were incubated for 90 min at 37°C in the presence of [^{125}I]EGF (100 000 c.p.m., 900 000 c.p.m./ng) and either EGF or EGF–FITC (0.1–500 ng/ml). The cells were then washed four times with DMEM containing 0.1% BSA and 0.02% sodium azide and were solubilized in 1 ml 0.5 M NaOH. Radioactivity was determined using a Packard Model 500C gamma counter.

Mitogenic activity was demonstrated using BALB/c 3T3 mouse fibroblasts as described elsewhere (Burgess *et al.*, 1983).

The ability of EGF or EGF–FITC to induce the formation of colonies of NRK in soft agar was performed as described by Roberts *et al.* (1980) in the presence of maximal levels of TGF_β prepared from bovine kidneys (Roberts *et al.*, 1983).

Acknowledgements

We are grateful to Katja Bizilj for technical assistance with the flow cytometric fluorescence measurements, to Kirsten Hoffmann for help with cell culture and Richard Simpson for the amino acid analysis and determination of the EGF–FITC concentration. Our thanks also to Sue Blackford who typed the manuscript. We would also like to acknowledge helpful discussions with Dr R.M.Böhmer.

References

Blatt,E., Chatelier,R.C. and Sawyer,W.H. (1984) *Chem. Phys. Lett.*, **108**, 397–400.

Burgess,A.W., Lloyd,C.J. and Nice,E.C. (1983) *EMBO J.*, **2**, 2065–2069.

Encinas,M.V. and Lissi,E.A. (1982) *Chem. Phys. Lett.*, **91**, 55–57.

Fabricant,R.N., De Larco,J.E. and Todaro,G.J. (1977) *Proc. Natl. Acad. Sci. USA*, **74**, 565–569.

Gill,G.N. and Lazar,C.S. (1981) *Nature*, **293**, 305–307.

Haigler,H., Ash,J.F., Singer,S.J. and Cohen,S. (1978) *Proc. Natl. Acad. Sci. USA*, **75**, 3317–3321.

Kawamoto,T., Sato,J.D., Le,A., Polikoff,J., Sato,G.H. and Mendelsohn,J. (1983) *Proc. Natl. Acad. Sci. USA*, **80**, 1337–1341.

Koeppe,P. and Hamann,C. (1980) *Computer Programs in Biomedicine*. **12**, 121–128.

Lifshitz,A., Lazar,C.S., Buss,J.E. and Gill,G.N. (1983) *J. Cell. Physiol.*, **115**, 235–242.

Rees,A.R., Gregoriou,M., Johnson,P. and Garland,P.B. (1984) *EMBO J.*, **3**, 1843–1847.

Roberts,A.B., Anzano,M.A., Meyers,C.A., Wideman,J., Blacher,R., Pan, Y.C.E., Stein,S., Lehrman,S.R., Smith,J.M., Lamb,L.C. and Sporn,M.B. (1983) *Biochemistry*, **22**, 5692–5698.

Roberts,A.B., Lamb,L.C., Newton,D.L., Sporn,M.B., De Larco,J.E. and Todaro,G.J. (1980) *Proc. Natl. Acad. Sci. USA*, **77**, 3494–3498.

Sklar,L.A. and Finney,D.A. (1982) *Cytometry*, **3**, 161–165.
Sklar,L.A., Finney,D.A., Oades,Z.G., Jesaitis,A.J., Painter,R.G. and Cochrane,C.G. (1984) *J. Biol. Chem.*, **259**, 5661-5669.
Steinkamp,J.A. and Kraemer,P.M. (1979) In Melamed,M.R., Mullaney,P.F. and Mendelsohn,M.L. (eds), *Flow Cytometry and Sorting*. John Wiley and Sons, NY, pp. 497–504.
Titus,J.A., Sharrow,S.A., Connolly,J.M. and Segal,D.M. (1981) *Proc. Natl. Acad. Sci. USA*, **78**, 519–523.
Walker,F. and Burgess,A.W. (1985) *EMBO J.*, **4**, 933–939.
Watson,J.V., Chambers,S.H,. Workman,P. and Horsnell,T.S. (1977) *FEBS Lett.*, **81**, 1, 179–182.
Zidovetzki,R., Yarden,Y., Schlessinger,J. and Jovin,T.M. (1981) *Proc. Natl. Acad. Sci. USA*, **78**, 6981–6985.

Received on 21 February 1986